Intraspecific chemical variation of *Tanacetum vulgare* at plant and plot level affects plant growth and reproductive traits in field plant communities

Lina Ojeda-Prieto[1], Pamela Medina-van Berkum[2], Sybille Unsicker[2], Robin Heinen[1], Wolfgang W. Weisser[1]

[1] Terrestrial Ecology Research Group, Department for Life Science Systems, TUM School of Life Sciences, Technical University of Munich, 85354 Freising, Germany.

[2] Department for Biochemistry, Max Planck Institute for Chemical Ecology, 07745 Jena, Germany.

Author for correspondence: Lina Ojeda-Prieto (lina.ojeda@tum.de)

Abstract

Intraspecific plant chemodiversity plays a fundamental role in interactions between plants and their interaction partners. Individuals of a plant species can be clustered into chemotypes by dominant chemical compounds or their chemical composition. Intraspecific stands of plant communities can vary in the number and type of plant chemotypes that grow in them (i.e., chemotype richness). Chemotypic diversity at the stand level is a special case of intraspecific diversity that is predicted to increase stand-level ecosystem functioning. Here we describe a biodiversity experiment in which we manipulated intraspecific plant chemodiversity at the plot level using six different chemotypes of common tansy (*Tanacetum vulgare* L., Asteraceae). We tested the effects of chemotype identity and plot-level chemotype richness (1-6) on plant growth and reproductive traits under field conditions. We found that plant chemotypes differed in growth and reproductive traits, both at the plant level, and at the plot level, and that reproductive plant traits and plot-level trait means were affected by tansy chemodiversity. The plot-level trait means were influenced by the presence or absence of certain chemotypes in a plot. The community's headspace terpenoid blend minimally reflected plot-level leaf terpenoid compound blends. Although tradeoffs between chemodiversity and growth and reproductive traits were observed, the links between chemodiversity and traits expressed themselves in the early establishment but dissolved over time, suggesting that different chemotypes adopt different growth strategies, which may facilitate their establishment in nature. This long-term field experiment will allow for further investigation of the consequences of intraspecific chemodiversity for plant-insect interactions and insect community assembly.

Keywords: intraspecific diversity, tansy, *Tanacetum vulgare*, terpenoid, plant-plant competition, complementarity, functional traits, chemodiversity

Introduction

Individuals of the same plant species can express a staggering variation in phenotypes, including growth, reproductive and phytochemical traits (Raffard *et al.,* 2018; Siefert *et al.,* 2015; de Bello *et al.,* 2011; Fridley & Grime, 2010; Bolnick *et al.,* 2003). This variation within plant species is a major element in individual performance and population-, community- and ecosystem-scale processes (Westerband, Funk & Barton, 2021; Guisan *et al.,* 2019; Siefert *et al.*, 2015; Violle *et al.,* 2012). Functional traits are attributes of species that can be measured at the individual level and are related to their response to environmental conditions (via fitness) and impact ecosystem properties and ecosystem functioning (Isbell *et al.*, 2011). In addition to visible functional traits, plants can vary highly in their less apparent traits, such as chemical composition (Wetzel & Whitehead, 2020). For instance, many plant species show intraspecific differentiation in specialized metabolites along environmental gradients (Bakhtiari *et al.*, 2019; Moore *et al.*, 2014) or even at finer spatial scales, such as plant patches located in areas less than a few square kilometers (Kleine & Müller, 2011). Variation in chemical diversity has recently gained increased attention in ecology (Wetzel & Whitehead, 2020; Müller *et al.,* 2020).

Individuals of a plant species can be clustered into distinct groups - also called chemotypes - using their dominant compounds, the composition of volatile and non-volatile compound blends, or by comparisons of specific specialized metabolites produced by individuals (Eilers, 2021). The consequences of specialized metabolites for intra- and interspecific interactions have been studied in various plant model systems (Moore *et al.*, 2014), including *Tanacetum vulgare* (Neuhaus-Harr *et al.,* 2023; Eilers *et al.,* 2021; Clancy *et al.,* 2016; Kleine & Müller, 2011), *Jacobaea vulgaris* (Kostenko & Bezemer, 2013), *Plantago lanceolata* (Wurst *et al.,* 2008; Harvey *et al.,* 2005), *Senecio inaequidens* (Cano et al., 2009), and *Brassica oleracea* (Bustos-Segura *et al.,* 2017; Kos *et al.,* 2011; Kabouw *et al.,* 2010; Poelman *et al.,* 2009). Many specialized compounds can be emitted as volatiles shaping the assemblage and interactions, for instance, within the plant-associated insect community (Ponzio *et al.,* 2013). Although ecologists are beginning to understand the consequences of plant chemodiversity for plant-insect interactions, much less is known about how chemical diversity affects plant-plant interactions (Thorpe *et al.,* 2011).

Plants can display intraspecific chemodiversity at different levels. At the plant level, the phytochemical profile produced by different individuals of the same species is used to assign them to specific chemotypes. Intraspecific chemodiversity can also manifest at the population, stand, or plot level (Clancy, 2021; Eilers, 2021; Müeller *et al.,* 2020; Clancy *et al.,*

2018; Seft, Weisser & Zytynska*,* 2017). Here, intraspecific chemodiversity is represented by the richness (i.e., the number of chemotypes) and relative abundance of different chemotypes of the same plant species that interact in the same space. While plant chemodiversity varies across levels, i.e., within individuals, among individuals within populations, and among populations, how variation in plant- and plot-level chemodiversity affects plant functional traits related to their growth and reproduction is still largely an open question.

The effects of increasing plant diversity on processes at the ecosystem level have been intensively studied in the framework of biodiversity-ecosystem functioning research (Weisser *et al.,* 2017; Chapin *et al.*, 1992). In most of the work, manipulation of plant diversity was achieved by creating plant communities that differed in the number of plant species they contain. In contrast to the wealth of studies manipulating plant community diversity at the plant species level, there are far fewer studies where plant community diversity is manipulated at the within-species level, i.e. by creating plant communities with the same number of plant species, but with different extent of intraspecific variation. In a seminal study, (Crutsinger *et al.*, 2006) showed that in one-species *Solidago altissima* communities that differed in the number of *Solidago* genotypes they contained, increasing genotypic diversity increased arthropod community species richness and also increased plant community biomass. The number of studies manipulating intraspecific diversity of plant communities has been increasing in the past years (Raffard *et al.*, 2019; Koricheva & Hayes, 2018; Genung *et al.*, 2012). However, the detailed results differ between studies and taxa, even if one focuses just on effects on herbivores (Bustos-Segura *et al.,* 2017; Barton *et al.*, 2015). A general trend is that increased intraspecific diversity of the plant community increases the diversity of the associated arthropod community, and that effects on natural enemies of herbivores are generally higher than effects on the herbivores themselves, suggesting changes in top-down control (see meta-analysis in Koricheva *et al.*, 2018; Hauri *et al*. 2021; Fernandez-Conradi *et al*. 2022; Hauri *et al*. 2022). The mechanisms underlying these effects are still being discussed. In plots differing in genotypic diversity, some effects on the herbivore community were found to be due to changes in plant size that varied both with genotype identity and with the particular genotypic composition of the plant community (Bustos-Segura *et al.,* 2017; Genung, 2012). In addition, there were effects of genotypic identity on the herbivore community that were not mediated by plant size (Bustos-Segura *et al.,* 2017; Genung, 2012).

Plants in highly intraspecifically diverse communities might experience tradeoffs in their fitness because of competition with neighboring conspecifics (Ziaja & Müller, 2022; Viola *et*

al., 2010). Furthermore, plants may experience increased intraspecific competition with other plants by releasing allelochemicals affecting nutrient uptake, growth rate, survival, and seed germination (Mahdavi-Arab *et al.*, 2014). They may, however, also experience reduced competition due to niche partitioning because of differences in functional traits leading to different growth strategies (Gallien, 2017). Thus, the intraspecific chemodiversity of plants growing in an environment might also affect the performance of plants growing there.

The terpenoid compounds stored in leaves play a critical role in plant interactions (Clancy *et al.,* 2016). For example, some of the specialized metabolites, stored in anatomical reservoirs in leaves, can be released by a plant in a volatile form either because of their chemical properties (volatility and solubility) or due to the plant's physiological or morphological properties (such as the presence of trichomes; see He *et al.,* 2011; Aschenbrenner *et al.,* 2013; Gershenzon & Dudareva, 2007). Although volatile production is hard to accurately predict (Dicke, Van Loon & Soler, 2009; Dudareva *et al.,* 2006), it is plausible that the volatile headspace profile will be related to the compounds found and stored in leaves. However, emitted volatile profiles might also differ from the ones stored in oil reservoirs of trichomes because some specific volatile organic compounds are produced only upon attack (known as herbivore-induced plant volatile -HIPV-, Rashid & Chung, 2017) or can be induced under abiotic or biotic stress (like green leaf volatiles, benzenoids, and terpenoids). For example, Clancy and collaborators (2016) found that emitted *T. vulgare* headspace volatiles differed from compounds found in leaves at the individual level by 82%. However, to which extent the chemotype richness and stored chemical profiles of a group of plants affect the blend of volatiles in their communal headspace remains poorly understood.

Here, we designed a field experiment using *Tanacetum vulgare* L. (Asteraceae), in which we manipulated plot-level chemotype richness and the presence of particular plant chemotypes within the plots, to test the effects on plant growth and volatile emission. *Tanacetum vulgare* exhibits a high intraspecific variation in specialized metabolites (Bálint *et al*., 2016; Rohloff, Mordal & Dragland, 2004), mainly mono- and sesquiterpenes (Ziaja & Müller, 2022; Keskitalo, Pehu & Simon, 2001), and is easy to propagate clonally (Bálint *et al*., 2016). Moreover, intraspecific chemodiversity of *T. vulgare* occurs in different geographical regions and within populations, meaning that plant-plant interactions of distinct chemotypes often occur in close proximity in nature (Clancy *et al.*, 2016; Kleine & Müller, 2011).

We measured growth and reproductive traits over two growing seasons and sampled headspace volatiles to test the following hypotheses:

(1) at the individual plant level, chemotypes will differ in growth and reproductive traits, and

these will be affected by the plot-level chemical richness of the plots they grow in.

(2) at the plot level, higher plot-level chemotype richness will increase plant growth, in line with the generally observed positive effects of biodiversity in the ecological literature.

(3) individual chemotypes will differ in their effect on plot-level effects.

(4) plant communities with higher plot-level chemotype richness will display a more chemically diverse headspace blend than plots with lower plot-level chemotype richness.

Materials and methods

Chemotypic characterization of tansy lines and biological replicates

We used established chemotypes that were also used in Neuhaus-Harr *et al.* (2023), where plant chemotyping and chemotype selection is described in great detail. For terpenoid composition, see Fig S1.

Propagation of plant material for the field experiment

Stem parts from the 18 selected daughters were trimmed and used to produce 27-40 cuttings per daughter. Individual cuttings were cut 1-2 cm below and 4-5 cm above a leaf node. The leaf size was reduced by 60% to reduce evapotranspiration and improve the survival rate by shortening and trimming the leaflet. Stem cuttings were placed into seedling trays with soaked potting substrate and protected with a clear plastic propagation cover. After three weeks and root and shoot formation, the cover was gradually opened to allow the cuttings to acclimate. As the cuttings grew, they were transplanted into 10 cm pots and later into 17 cm pots before transplanting in the field site in May 2021. Potted plants were automatically watered from the bottom up and fertilized with Universol Blue fertilizer ® (18%N - 11%P - 18%K; ICL Deutschland, Nordhorn, Germany). During propagation and growth, plants were not treated with chemical insecticides or fungicides, but we applied biological control where needed. At the end of the growing period, there were multiple cloned plants from each of the 18 daughters. Thus, for each chemotype, there were cloned plants from each of three daughters that could be used in the experimental design.

Experimental design

The field experiment took place in the Jena Experiment site located on the floodplain of the Saale River in Jena, Germany (50°55’N, 11°35’E, 130 m.a.s.l., Weisser *et al.*, 2017). In May

2021, weeds were removed, and soil was tilled. The field was divided into 84 plots (1 x 1 m) separated from each other by 70 cm footpaths and distributed in 6 replicated blocks (Fig. 1c). No fertilizer and no chemical insecticides or fungicides were used, and weeds were removed by hand every two weeks during the growing season.

We created plots of six tansy plants that were evenly distributed around a 70 cm diameter circle (84 plots x 6 plants = 504 plants total; Fig. 1a). The design followed suggestions of the design for biodiversity experiments: each plot differed in the number and identity of tansy chemotypes assigned to them. The number of different chemotypes in one plot (hereafter: plot-level chemotype richness) ranged from 1, 2, 3, to 6 (Fig. 1b). For instance, a plot with a plot-level chemotype richness of 1 was assigned six plants of the same chemotype. Within the plot, we maximized the number of daughters per chemotype. Daughters from each chemotype were equally distributed over the different treatment plots where possible, and structurally assigned where the equal division was not possible (e.g., in the case of shortage of plants of one daughter, they were replaced with a randomly picked daughter of the remaining two daughters of the same chemotype). So, a plot with plot-level chemotype richness 1 was assigned 2 clones from each of the three daughters of the plot chemotype, for plot-level chemotype richness 2 there was one clonal plant of each of the three daugthers of each of the two chemotypes in the plot etc. Lastly, a plot with plot-level chemotype richness 6 was assigned one clonal plant from one daughter of each of the six different chemotypes.

Each plot's plot-level chemotype richness composition was *a priori* assigned - before in-depth analysis of the chemotype terpenoid composition - to avoid biases favoring the presence of one chemotype over another. Each unique chemotype combination was thus replicated twice, except for plot-level chemotype richness level 6, which was replicated twelve times, but with different daughters. Hence, our field experiment contained 12, 30, 30, and 12 replicate plots for plot-level chemotype richness levels 1, 2, 3, and 6, respectively. Plots were distributed equally in six randomized blocks. Each block consisted of 14 plots: two plots of chemotype richness level 1, five plots of chemotype richness level 2 and 3, and two plots with chemotype richness level 6 (Fig. 1c). Appendix 1 offers an overview of the exact assignment of daughters to plots.

Plant morphological trait measurements

We measured six morphological plant traits for individual plants, including four growth traits (the number of stems per plant, the height of the highest stem, and fresh and dry above-ground biomass) and two reproductive traits (the cumulative number of flower heads and the

flowering index).

In 2021, we counted the number of stems that were larger than 5 centimeters above the ground, and measured plant height as the distance between the longest stem and the ground, without stretching out leaves, in total three times (June 01, June 22, and October 28).

As a measure of phenology, we counted and cut off all ripe flowerheads weekly during the whole season in 2021 (from June 01 to October 28). Flowerheads were cut off to avoid a re-seeding of plots with new plants. At the end of the season (October 28, 2021), we obtained dry biomass of each plant; plants were cut off 5 cm above the ground, placed in single paper bags, and dried for 72 hours at 60°C in a drying room (Thermo Scientific) of the University of Jena facilities.

In 2022, we counted the number of stems once (July 06) and measured plant height three times (May 14, July 06, and October 05). The phenological status of each stem of each plant was determined once (on July 06) using six categories: No flowering stem [1]; Developing closed flowering stem [2]; Developing open flowering stem [3]; Unripe flowering stem [4]; Ripe flowering stem [5]; Stem with mature seeds [6] (Fig. 1e). For obtaining a measure of phenology at the plant level, we calculated a flowering index for each plant by dividing the sum of stem level flower indices by the number of stems. To obtain a measurement at the plot level, we average plant-level flower indices per plot.

At the end of the second season, all plants were again cut off 5 cm above ground but immediately weighted in the field to obtain fresh biomass (October 05, 2022). From this we calculated both plant-level as well as plot-level biomass.

Headspace collection

Headspace volatile organic compound emissions were collected at the plot level (including all six individual plants), between May 12 and 14, 2022, using a closed-push-pull system for 2 hours (Fig. 1f). Weeds were removed by hand from the plots 10 days before the measurements, to reduce the collection of volatiles from plants different from tansy. In addition, one extra new plot was prepared by completely cleaning out the plant material 10 days before and used as a volatile background profile (red plot in Fig. 1c).

For collection, a squared bag made from odorless PET (110 cm x 110 cm x 40 cm) was installed covering the whole plot. Air entered the system after passing through an activated

charcoal filter at a flow rate of 1.5 L/min and was pumped out through a trap at a rate of 1 L/min. The trap contained 25 mg of Poropak-Q absorbent (Volatile Collection Trap (VCT) LLC, USA) (Fig. 1f). VOCs were collected over a period of three days with three rounds of ten plots per day (two full blocks + two background plots = 30 plots per day). Plots were assigned beforehand to ensure each plot-level chemotype richness level and the bare-soil plot were included in each round.

After VOC collection, the traps were eluted with 200µl dichloromethane containing nonyl acetate as an internal standard (SigmaAldrich, 10 ng µl-1). VOCs were analyzed with using a a Hewlett-Packard model 6890 gas chromatograph coupled to a Hewlett-Packard model 5973 mass spectrometer (GC-MS). The GC was operated with helium as carrier gas at 1 ml/min, splitless injection (injection temperature: 220 °C, injection volume: 1 µl), a DB-5MS column (30 m × 0.25 mm, 0.25 µm film, J & W Scientific, Folsom, CA, USA), and a temperature program from 40 °C (2 min hold) to 350 °C (2 min hold) with a first gradient of 7 °C min^{-1} to 155 °C, and a second gradient of 60 °C min^{-1} to 300 °C. The GC was coupled to a single quadrupole mass spectrometer (Hewlett-Packard model 5973) operated in electron impact ionization mode. Transfer line temperature was 270 °C, the ionization potential was 70 eV, and a scan range of *m/z* 40–350 was employed.

VOCs were identified by comparing retention times and mass spectra with commercial standards (when available), and by comparison to the mass spectral libraries Wiley 275 (Wiley and National Institute of Standards) and NIST05a (National Institute of Standards and Technology, Gaithersburg, MD). We verified the VOC identity by calculating Kovats retention indices. The qualitative and quantitative analysis of the volatile data is beyond the scope of this study, here we report only on volatile terpenoid diversity metrics at the plot level.

Statistical analysis

All analyses were performed in R version 4.2.2 and RStudio 2022.07.2+576 (R Core Team, 2021).

To analyse plot-level chemotype richness, we calculated plot-level diversity metrics using the '*chemodiv*' package (Petrén, Köllner & Junker, 2023). Note that we calculated theoretical chemotype diversity metrics based on the cumulative terpenoid profiles of each respected daughter present in a plot and calculated realized volatile diversity metrics based on our volatile collection at plot level. Data was visualized using the '*ggplot2'* package (Wickham, 2016).

All analysis on plant- and plot-level effects of chemodiversity on plant traits were analyzed using mixed-effect models by means of the '*lme4*' package (Bates *et al.*, 2015). P-values were estimated by type II Wald-Chi-Squared tests using the '*car'* package (Fox & Weisberg, 2019). After fitting a model, *post hoc* pair-wise comparisons among factor levels were assessed with the '*emmeans'* package with Tukey adjustment (Russell, 2021). We distinguished between plot-level and plant-level analyses, as described below.

All variables were analyzed separately for each time point.

Chemotype and plot-level chemotype richness effects on traits of individual plants

To test the effects of chemotype and plot-level chemotype richness on traits of individual plants, both factors and their interaction were included as fixed factors in Generalized Linear Mixed-Effect Models (GLMM) with Poisson distribution for counting data (number of stems for both years and the cumulative number of flower heads) and Linear Mixed-Effect Models (LMER) for the other individual plant traits (plant height, flowering index, and square root transformed dry above-ground biomass and square root transformed fresh above-ground biomass). Note that we treated chemotype richness as a continuous variable with one degree of freedom. Random effects were Daughter ID to account for technical replication of each daughter via cuttings and either Plot ID (84 in total) nested in Block ID (for the number of shoots on October 28, 2021, and, except for height on May 14, 2022, all measurement of height) or Block ID (for the rest of variables). If the effect of a factor was significant, *post hoc* pair-wise comparisons with Tukey adjustment were conducted to assess significant differences between factor levels.

Chemotype presence and plot-level chemotype richness effects on plot-level measurements

To test the effects of chemotype and chemotype richness on average plot-level plant traits, we first averaged each plant trait at the plot level (Community weighted means accounted for abundance), except for the flowering index.

To test the effect of the presence/absence of a chemotype on plot-level trait values, we carried out a separate analysis per chemotype. This was done by running a linear model with Block ID plus plot-level chemotype richness and chemotype presence (which indicates if a specific chemotype is present or not in the plot) and their interaction as fixed effects, separately for each chemotype.

Plot-level theoretical leaf and realized volatile chemodiversity metrics

We calculated chemodiversity metrics at the plot level based on the leaf terpenoid profiles before planting (plot-level theoretical leaf chemodiversity), headspace terpenoid measurements in the field (plot-level realized volatile chemodiversity). Plot-level theoretical leaf chemodiversity metrics were calculated by summing up the absolute leaf terpenoid concentrations (nmol/g) produced by each of the six specific daughters present in each plot. Those absolute leaf terpenoid profiles were obtained from the chemical analysis performed on leaves from greenhouse plants in 2020 before making the cuttings and planting them in the field. Then, we calculate plot-level theoretical leaf terpenoid richness, concentration, Hill Shannon index, and Hill evenness (Petrén *et al.,* 2022). Plot-level realized volatile chemodiversity metrics were calculated based on the plot-level absolute terpenoid emissions (ng/h) detected by headspace VOC collection.

As plants were chemotyped *a priori* to transplanting them to the field and were not affected by field conditions, plot-level theoretical leaf chemodiversity was analyzed by linear models with plot-level chemotype richness as the independent variable, without any random factors. Plot-level realized volatile chemodiversity metrics based on field-collected headspace terpenoids were analyzed by linear models with plot-level chemotype richness as the independent variable and Block ID (6 in total) and Collection Day ID (3 in total) as random factors.

Results

Field establishment

The establishment of the field experiment was successful; all 504 plants survived until the first seasonal harvest date (October 28, 2021). By early May of the second year (May 2, 2022), 96.6% of the plants (487 of 504 plants) showed shoot regrowth. Of these 487 plants, 4 more plants, which had shown some above-ground growth, were naturally eliminated and were not present at the harvest date of the second year (October 05, 2022). Missing data were excluded from analyses of plant traits at the plant level for each respective time point. In total, 18 plants were reported as absent for the first (May) measurements. In total, 20 plants were missing for the second (July) measurements. In total, 21 plants for the final measurements (October). Due to regrowth and mortality the missing plants between time points only have a partial overlap. Plot-level averages were calculated according to the number of plants registered in the plot at the measurement date.

Chemotype and plot-level chemotype richness effects on individual plants

We used analyses separated for each time point to assess the effect of chemotype and plot-level chemotype richness across and between seasons.

The number of stems of a plant was significantly affected by plant chemotype identity on June 22, 2021 (χ^2_5 = 21.54, p <0.001, Fig. 2a). *Post hoc* analyses revealed that in the 2021 season, the Cam7 chemotype had the highest number of stems compared with all other five chemotypes (Fig. 2a). However, the effects of chemotype on the number of stems across chemotypes was not stable across nor between growing seasons (Table S1 and Fig. S2). Differences in the number of stems across chemotypes were less pronounced towards the end of the first season (Fig. S2) and became even less distinct for 2022 (χ^2_5 = 3.09, p = 0.686, Fig. 2d).

With respect to plant height, chemotypes were only marginally significantly different on June 22, 2021 (χ^2_5 = 10.54, p = 0.061, Fig. 2b), but were when harvesting on October 28, 2021 (χ^2_5 = 12.26, p = 0.031, Table S2). At this time point, several outliers where there was no ecological reason for exclusion caused deviation from a normal distribution that could not be solved with transformation. Therefore, for this time point, the chemotype effect must be interpreted with some caution. For instance, even though chemotype had a significant effect (χ^2_5 = 12.26, p = 0.031), a *post hoc* test for October 28, 2021, did not reveal differences in height across chemotypes. Moreover, any effect of chemotype on height was not kept by 2022 (χ^2_5 = 1.58, p = 0.903; Fig. 2e, Fig. S3). The above-ground biomass of the Aue41 chemotype was slightly higher in both growing seasons, although the effect of the chemotype was not significant (dry above-ground biomass 2021: χ^2_5 = 9.35, p = 0.096, Fig. 2c; fresh above-ground biomass 2022: χ^2_5 = 2.65, p = 0.753, Fig. 2f).

There was no significant effect of plot-level chemotype richness nor the interaction between chemotype and plot-level chemotype richness for any of the growth traits measured on individual plants, except for a small effect of plot-level chemotype richness on the number of stems (χ^2_1 = 6.86, p = 0.009, Fig. 2d).

Reproductive plant traits were significantly affected by plant chemotype (Table S3, S4), both in terms of the cumulative number of flower heads (χ^2_5 = 29.44, p <0.001) and flowering phenology (χ^2_5 = 51.34, p <0.001). Interestingly, reproductive plant traits depended on both chemotype and the plot-level chemotype richness, as indicated by an interaction between the two factors (cumulative number of flower heads: χ^2_5 = 1043.06, p <0.001; flowering index: χ^2_5 = 15.16, p = 0.010). For example, the Aue41 chemotype produced more flower heads in plots with higher plot-level chemotype richness in the first growing season. The other five chemotypes produced fewer flower heads in plots with higher plot-level chemotype

richness (Fig. 2g). The Cam7, Spar11B, and Schie5 chemotypes showed more advanced flowering phenology (i.e., higher flowering index) in plots with higher plot-level chemotype richness. In contrast, the Aue41, Saal2, and Schienen3 chemotypes showed more advanced phenology in plots with lower plot-level chemotype richness (Fig. 2h). Overall, the number of flower heads was also significantly lower in plots with higher plot-level chemotype richness ($\chi^2_1 = 123.54$, $p < 0.001$).

Chemotype presence and plot-level chemotype richness effects on plot-level measurements

The presence or absence of certain chemotypes in a plot affected plot-level variables related to plant growth, i.e., number of shoots, height, dry biomass, and to reproduction, i.e., cumulative number of flower heads. However, the effects of particular chemotypes were variable and differed with time in the growing season (Figs. S5-S8).

In 2021, only two chemotypes had significant effects on the mean number of stems per plot, i.e., Cam7 and Schienen3, and only in one sampling time point (July 22, 2021). In this time point, the average number of stems at the plot level significantly increased when Cam7 was present ($F_{1,75} = 10.35$, $p = 0.002$, Fig. 3a). The Cam7 chemotype was also the chemotype that had the highest number of stems in 2021 (Fig. 2a). The presence of the Schienen3 chemotype lowered the number of stems at the plot level ($F_{1,75} = 8.10$ $p = 0.006$, Fig. 3a). The effect of the presence/absence of the Cam7 or Schienen3 chemotypes did not differ across chemotype richness levels, indicated by the absence of interactions (Table S5). In 2022, chemotype presence/absence patterns on stem number were slightly different. Although we did not find a significant main effect of the presence/absence of any of the chemotypes on the number of stems, we did observe an interaction between plot-level chemotype richness and the presence of the Cam7 chemotype ($F_{1,75} = 4.29$, $p = 0.042$, Fig. 4a). In plots where the Cam7 chemotype was present, the number of stems did not differ, whereas, in its absence, the number of stems decreased sharply with increasing plot-level chemotype richness. Across all six chemotype-specific models, and in all time points in both years, plot-level chemotype richness had marginally significant negative effects on the mean number of stems per plot (Table S5).

In 2021, the presence of the Aue41 chemotype increased the mean height at plot-level ($F_{1,75} = 14.41$, $p < 0.001$, Fig. 3b). Aue41 was comparatively high (Fig. 2b), which drove this effect. In contrast, the mean plot-level height decreased (any time point in 2021, Fig. S7) when the Cam7 chemotype was present ($F_{1,75} = 25.18$, $p < 0.001$). The presence of the Saal2 chemotype also lowers the plot-level average height ($F_{1,75} = 5.54$, $p = 0.021$), and the effect was stronger in low plot-level chemotype richness when it was present and in high plot-level

chemotype richness when it was absent, as indicated by a marginally significant interaction between plot-level chemotype richness and chemotype presence ($F_{1,75} = 3.80$, $p = 0.055$). In 2022, only the presence of Spar11B chemotype lowered the mean plot-level height, but only in the May 14, 2022 sampling point (Fig. S6, Fig. S8, Table S6). We observed no effects of plot-level chemotype richness on mean plot-level height at any time point in any year (Table S6).

In 2021, dry mean above-ground biomass strongly increased when the Aue41 chemotype was present in the plot ($F_{1,75} = 59.54$, $p < 0.001$, Fig. 3c). Similarly, but more smoothly, fresh above-ground also increased when the Aue41 chemotype was present in 2022 ($F_{1,75} = 10.70$, $p = 0.002$, Fig. 4c). The presence of the Schie5 chemotype reduced the mean dry above-ground biomass at the plot level ($F_{1,75} = 9.89$, $p = 0.002$) was greater than the effect found on the fresh biomass for the year 2022 ($F_{1,75} = 7.24$, $p = 0.009$). In both cases, the presence of the Schie5 chemotype reduced mean above-ground biomass.

The presence of Aue41 in plots affected the average plot-level number of flower heads positively ($F_{1,75} = 13.08$, $p < 0.001$, Fig. 3d), as Aue41 chemotype produced the highest amount of flower heads in the first growing season. Presence of the Saal2 negatively affected the mean number of flower heads ($F_{1,75} = 12.12$, $p < 0.001$). We also observed an interactive effect between presence of Aue41 and plot-level chemotype richness ($F_{1,75} = 5.25$, $p = 0.025$), between presence of Cam7 and plot-level chemotype richness ($F_{1,75} = 4.98$, $p = 0.029$), between presence of Schienen3 and plot-level chemotype richness ($F_{1,75} = 7.08$, $p = 0.010$), and between presence of Spar11B and plot-level chemotype richness ($F_{1,75} = 9.60$, $p = 0.003$). In all the interactions, plot-level chemotype richness negatively affected flower number negatively when the chemotypes were absent, but not when they were present (Fig. 3d, Table S7).

For the second growing season, the presence/absence of certain chemotypes strongly affected the flowering phenology in the models for the Aue41, Cam7, Schienen3, and Spar11B chemotypes (Table S8, Fig. 4d). The presence of the Cam7 or Schienen3 chemotype pulled up the flowering index, i.e., advanced flowering phenology of the whole plot compared to the plots where they were not present (Cam7 chemotype presence: $F_{1,75} = 37.90$, $p < 0.001$; Schienen3 chemotype presence: $F_{1,75} = 5.88$, $p = 0.018$). Conversely, plot-level flowering phenology was pulled down, i.e., flowering phenology was less advanced when the Aue41 or Spar11B chemotype was present than when it was not (Aue41 chemotype presence: $F_{1,75} = 16.27$, $p < 0.001$; Spar11B chemotype presence: $F_{1,75} = 22.42$, $p < 0.001$).

Diversity metrics

A linear regression was used to test whether plot-level chemotype richness correlated to diversity metrics based on the plot-level leaf terpenoid and the plot-level headspace terpenoid profiles. The overall regressions with plot-level chemotype richness were statistically significant for plot-level leaf terpenoid richness ($F_{1,82}$ = 20.48, R^2 = 0.20, p <0.001, Fig. 5a), plot-level leaf terpenoid Shannon diversity ($F_{1,82}$ = 37.25, R^2 = 0.31, p <0.001, Fig. 5b), and plot-level leaf terpenoid Hill evenness ($F_{1,82}$ = 31.78, R^2 = 0.28, p <0.001, Fig. 5c) and all diversity metrics increased when the plot-level chemotype richness increased. In contrast, the relationship between plot-level chemotype richness and plot-level total leaf terpenoid concentration was not significant ($F_{1,82}$ = 0.00, R^2 = 0.00, p = 0.967, Fig. 5d). Remarkably, plot-level chemotype richness had no significant relationship with the diversity metrics based on the headspace terpenoid profiles. Plot-level headspace terpenoid richness (χ^2_1 = 0.36, R^2 = 0.00, p = 0.546, Fig. 5e), plot-level headspace total terpenoid emission (χ^2_1 = 0.02, R^2 = 0.00, p = 0.897, Fig. 5f), plot-level headspace terpenoid Hill Shannon index (χ^2_1 = 1.60, R^2 = 0.02, p = 0.206, Fig. 5g), and plot-level headspace terpenoid Hill evenness (χ^2_1 = 0.08, R^2 = 0.00, p = 0.780, Fig. 5h) all not correlate with the plot-level chemotype richness and the model's total variance explained (R^2 values) is very limited.

Headspace terpenoid analysis

The headspace VOC collection led to the identification of 60 compounds. Volatile organic compounds were classified into five major classes: green leaf volatiles (GLV), monoterpenes, sesquiterpenes, alkanes, and others. The distribution of those classes did not shift when plot-level chemotype richness changed (Fig. S8). Terpenoids represented the most abundant and diverse of the compounds in the bouquet (84% of the compounds), followed by GLV with 15% (Table S9). For comparison purposes, only known headspace terpenoids were considered.

A total of 44 terpenoids were detected by hexane extraction from leaf material and 49 terpenoids in the headspace of tansy communities. It resulted in 27 terpenoids uniquely identified in the headspace of tansy communities (41.5%), 16 terpenoids solely identified on tansy leaves (24.6%), and 22 terpenoids identified by both methods (33.8%), i.e., headspace VOC collection and hexane leaf extraction (Table S9).

Discussion

Here, we designed a biodiversity field experiment with *Tanacetum vulgare*, in which we

manipulated intraspecific chemodiversity at the plot level, and studied how chemodiversity affects plant performance in the first two years after establishment. Our study showed that chemotypes differed in all studied morphological traits but that effects of plot-level chemotype richness were only found on reproductive traits and not growth traits. The presence and absence of certain chemotypes and the plot-level chemotype richness influenced plot-level functional traits. Nevertheless, the influence of both factors on functional traits seemed to level off over time. We found that the plot-level headspace terpenoid profiles reflected the theoretical plot-level leaf terpenoid profiles, but only to a limited extent. Lastly, we observed relationships between chemodiversity and plant performance that changed over time.

We found that tansy chemotypes vary in growth plant traits (number of stems and height) and reproductive traits (number of flower heads and flowering phenology) under field conditions. These findings broadly support the work of previous studies that used the same plant model system and found links between plant chemotypes and plant traits (Neuhaus-Harr *et al.,* 2023; Keskitalo, Pehu & Simon, 2001). For instance, tansy chemotypes with a high concentration of camphor also were the tallest compared with other chemotypes rich in *trans*-thujone, artemisia ketone, 1,8-cineole, or davadone-D; and chemotypes rich in artemisia ketone or davadone-D produced more flower heads and flowered later compared with the other four chemotypes (Keskitalo, Pehu & Simon, 2001). However, these findings are not completely comparable to ours since Keskitalo *et al.* (2001) analyzed the effect of chemical composition on certain traits at a wider geographic scale, and the chemotypes used by them and the ones used here are different in their chemical composition.

Contrary to our hypothesis, no differences were found in plant growth parameters when plants grew in plots that differed in plot-level chemotype richness, indicating that the morphology of each chemotype is consistent across the environments they grow in. Variability in growth traits across chemotypes may enable individuals to partition local resources into different growth strategies and avoid intraspecific competition (Gallien, 2017; Messier, McGill & Lechowicz, 2010). For instance, the Aue41 chemotype developed large biomass and typically few but tall and thick stems compared with other chemotypes such as Cam7, which developed more stems but shorter and slighter. Interestingly, however, the morphological differences between the different chemotypes converged over time, which not only emphasizes the role of different strategies for individual survival, particularly during early establishment but also aligns with intraspecific chemodiversity is another layer that allows plants to display different resource utilization patterns (Müller & Junker, 2022). Only the Aue 41 chemotype remained quite distinct in both years, possibly due to its pronounced

strategy of growing: tall and thick stems and high biomass.

In contrast to what we observed for growth traits, *T. vulgare* reproductive traits differed between chemotypes and depended on the plot-level chemotype richness. Although Moreira *et al.* (2016) and Hughes *et al.* (2008) suggested that plants in more diverse plots had higher individual plant fitness, all studied chemotypes, except for the Aue41 chemotype, were inhibited in plots with high plot-level chemotype richness more than they were in low-chemotype richness plots, at least in terms of the number of flower heads. It suggests that growth strategies that made the Aue41 chemotype very dominant in the first year in height and biomass might also bring some fitness advantages to the Aue41 chemotype in highly diverse plant communities. It also suggests that most *T. vulgare* chemotypes suffer in more chemically diverse environments, which contrasts with our expectations that such environments would benefit plants. This interpretation is made based on the effect of chemodiversity on plant traits. It differs from that of Ziaja & Müller (2023), who reported that specific *T. vulgare* chemotypes (e.g., dominated by artemisia ketone and α-thujone/ß-thujone) benefit from allospecific neighbors in high chemical diverse environments in terms of herbivore load of *Uroleucon tanaceti* and *Macrosiphoniella tanacetaria* aphids.

Another key finding was that intraspecific plot chemodiversity influences phenology in *T. vulgare*. In the case of the Aue41 chemotype, the effect of plot-level chemotype richness was positive on the number of flower heads but negative in the flowering index value. It appears that in different chemical environments, different *T. vulgare* chemotypes have different flowering strategies due to the effects of the chemical environment they grow in. For instance, the Cam7, Schie5, and Spar11B chemotypes had a more advanced flowering status at the time of assessment (high flowering index value) in plots with higher plot-level chemotype richness, while the Aue41, Saal2, and Schienen3 chemotypes had a more delayed phenology (low flowering index value) in such plots. We speculate that *T. vulgare* may be able to sense their neighboring plants, either through direct competition (e.g., for space and nutrients), via the perception of volatiles (Ninkovic, Markovic & Rensing, 2021; Ninkovic *et al.,* 2019; Kessler & Kalske, 2018; Karban, Yang & Edwards, 2014; Heil & Karban, 2010), or absorption of semi-volatile sesquiterpenoids emitted by neighboring plants (Himanen *et al.,* 2010). As a result, *T. vulgare* may avoid competition by being reproductively active at different times and optimizing their fitness. Variations in flowering phenology may also correlate with variations in interacting arthropod communities, which may affect reproductive success (Kuppler *et al.*, 2016). Moreover, differences in flowering phenology across chemotypes may constitute a strategy to avoid cross-pollination between certain tansy chemotypes that can result in poor seed production (Keskitalo, Lidén & Valkonen,

1998)

As predicted, plot-level trait values increased in 2021 because of the presence of certain chemotypes that had either more stems, were higher, had larger dry above-ground biomass, or produced more flower heads. In the same line, plot-level trait values decreased when chemotypes with fewer stems, smaller, lighter, or that produced fewer flowerheads were present. At the plot level, these individual chemotype contributions seem to become less pronounced over time, suggesting that the plots become more similar. This is important for future work investigating the role of chemodiversity on insect community assembly, as it reduces the strength of potential confounding effects of plant growth on insect community assembly and will help draw more robust conclusions and deepen our understanding of the consequences of chemodiversity.

In line with our predictions, most diversity metrics based on theoretical plot-level leaf terpenoid profiles increased with increasing plot-level chemotype richness. We observed no differences between plot types for the total approximate terpenoid concentration. In contrast to what we hypothesized; we found no effect of plot-level chemotype richness on diversity metrics calculated based on headspace terpenoids. Plots that were more diverse in terms of their leaf terpenoids were not necessarily more diverse in their plot-level headspace terpenoid profile. Headspace volatile terpenoids are part of the specialized metabolites a plant releases due to their chemical properties (e.g., volatility and solubility). They are frequently specific and strongly dependent not only on the constitutive specialized metabolite profile but also on biological, morphological, and chemical characteristics such as the abundance and type of interacting organisms above- and below-ground, plant age, and plant size (Kessler & Kalske, 2018; McCormick, Unsicker & Gershenzon, 2012; Takabayashi, Dicke & Posthumus, 1994). While the hexane extraction was performed from the leaves of young plants before planting them in the field in 2021, the headspace terpenoids were obtained in the spring season one year after planting (2022) under field conditions (where the plants interacted with each other and other organisms) and analyzed in a different lab. This could have led to changes in terpenoid diversity that may be reflected in our analysis (Eckert *et al.,* 2023).

Further research should be undertaken to investigate the qualitative changes in plot-level volatile composition and how they correspond to plot-level cumulative leaf terpenoid profiles, but this is beyond the scope of this study. Importantly, future investigations of leaf terpenoids and headspace terpenoids under field conditions over time, within and across growing seasons, upon induction, and in response to environmental stresses would help us

understand the temporal dynamics of plant terpenoid composition and volatile emission.

Producing and maintaining intraspecific chemodiversity of specialized metabolites can be costly (Kleine & Müller, 2013). Although their production and maintenance may be vital for their defensive function, it might also lead to tradeoffs between growth and defense (Zhou *et al.*, 2022; Herms & Mattson, 1992). The results of our study support the concept of tradeoffs between metabolic costs of terpenoid production and growth; negative correlations between leaf terpenoid diversity and evenness and height and biomass were found at the plant level, suggesting that plants with more complex defenses are limited in their growth. In contrast, positive correlations were observed between diversity and evenness and the number of *T. vulgare* stems per plant, suggesting that more diverse and even plants invest more in stem growth. At the plant- and plot- level, positive and negative correlations were observed between approximate total terpenoid concentration and flowering index and plant height, suggesting that plants with higher terpenoid concentrations show more advanced flowering but are limited in their height, which results in similar patterns at the plot level. Although increased total terpenoid concentration appeared to cause tradeoffs with plant growth in the first year, both at the plant and plot level, these patterns completely disappeared in the second year. This is important, as it emphasizes the role of trait differentiation as a form of niche partitioning, especially as young plants are establishing in the field. Specialized metabolites might represent an increased adaptive potential, particularly to perennial plants (Eilers, 2021), regulate plant development, and mediate plant interactions (Pang *et al.*, 2021; Ninkovic *et al.*, 2019) and stress resistance (Isah, 2019). Thus, a tradeoff between defense and growth is highly dependent on the identity and diversity of compounds and on the plant's mechanisms to reduce the cost of producing them (by either assigning new functions to those metabolites or reintegrating them into primary metabolism, Erb & Kliebenstein, 2020). Therefore, plants were better established and adapted to the field for the second year and, thus, less limited by resources, and possible tradeoffs were not detected.

Conclusion

A mechanistic understanding of biodiversity-ecosystem functioning requires the analysis of the role of not only species number and functional groups, phylogenetic diversity, and within-group variation in functional traits (Tilman *et al.*, 1997b). Our results provide important insights into the underlying processes through which intraspecific chemodiversity acts on plant growth and reproductive traits, and although this study focuses on plant traits, this established field experiment also raises the possibility of further studying the role of intraspecific chemodiversity in interactions between plants and associated interaction

partners, such as herbivorous insects and their natural enemies, and pollinators. Insect diversity and abundance are typically positively correlated with plant species diversity and interspecific diversity of functional traits (Junker, Blüthgen & Keller, 2015). However, the effect of intraspecific plant chemodiversity on shaping such interactions in the field has received limited attention to date (but see Bustos-Segura *et al.,* 2017). The findings of this study suggest that intraspecific chemodiversity might influence ecosystem properties such as primary productivity, resource use efficiency, ecosystem stability, and resilience. Given the degradation of morphological trait differences over time, this field experiment offers a unique opportunity to study the effect of chemodiversity by means of constitutive plant terpenoid profiles in nature.

Acknowledgments

We thank the staff at TUM PTC Dürnast, particularly Sabine Zuber and Petra Scheuerer, for providing excellent care during the plant propagation and preparation phase. We thank Caroline Müller and Elisabeth Eilers for chemotyping the plants, Anne Ebeling and Nico Eisenhauer for providing space within the Jena Experiment and allowing us to use core facilities under Gerlinde Kratzsch's guidance. We thank Nafiseh Mahdavi for her help in establishing the field experiment, Leonardo Moreno for his help in the maintenance of the plants and in collecting data on both years of the field experiment, and the Jena Experiment gardening staff for providing advice and help in the maintenance of the experiment. Many thanks to Beate Piecha, Annika Neuhaus-Harr, and other friends and colleagues who helped during the harvests. This study was funded by the German Research Foundation (DFG), project 415496540 (WE3081/40-1), as part of the Research Unit (RU) FOR 3000. We thank all members of the RU as well.

Conflict of interest

The authors declare no conflict of interest.

Contribution of authors

WWW conceived the original idea and designed the experiment. RH prepared the field experiment and propagation of plants. LOP, RH and WWW planted the field experiment. LOP collected all data and maintained the field experiment. LOP analyzed ecological data with input from RH and WWW. PMvB, SU and LOP prepared and executed volatile collection. PMvB chemically analyzed volatiles. LOP wrote the manuscript with input from RH and WWW. All authors contributed to the final version and approved final submission.

References

Bakhtiari, M., Formenti, L., Caggìa, V., Glauser, G., & Rasmann, S. (2019). Variable effects on growth and defense traits for plant ecotypic differentiation and phenotypic plasticity along elevation gradients. *Ecology and Evolution*, *9*(7), 3740-3755.

Bálint, J., Zytynska, S. E., Salamon, R. V., Mehrparvar, M., Weisser, W. W., Schmitz, O. J., & Balog, A. (2016). Intraspecific differences in plant chemotype determine the structure of arthropod food webs. *Oecologia*, *180*(3), 797-807.

Barton, K. E., Valkama, E., Vehviläinen, H., Ruohomäki, K., Knight, T. M., & Koricheva, J. (2015). Additive and non-additive effects of birch genotypic diversity on arthropod herbivory in a long-term field experiment. *Oikos*, *124*(6), 697-706.

Bates, D., Maechler, M., Bolker, B., & Walker, S. (2015). Fitting Linear Mixed-Effects Models Using lme4. *Journal of Statistical Software, 67*(1), 1-48.

Bolnick, D. I., Svanbäck, R., Fordyce, J. A., Yang, L. H., Davis, J. M., Hulsey, C. D., & Forister, M. L. (2003). The ecology of individuals: incidence and implications of individual specialization. *The American Naturalist, 161*(1), 1-28.

Bustos-Segura, C., Poelman, E. H., Reichelt, M., Gershenzon, J., & Gols, R. (2017). Intraspecific chemical diversity among neighbouring plants correlates positively with plant size and herbivore load but negatively with herbivore damage. *Ecology Letters*, *20*(1), 87-97.

Cano, L., Escarré, J., Vrieling, K., & Sans, F. X. (2009). Palatability to a generalist herbivore, defence and growth of invasive and native Senecio species: testing the evolution of increased competitive ability hypothesis. *Oecologia*, *159*, 95-106.

Chapin III, F. S., Schulze, E. D., & Mooney, H. A. (1992). Biodiversity and ecosystem processes. *Trends in Ecology and Evolution*, *7*(4), 107-108.

Clancy, M. V. (2021). *The Chemical Ecology of Tansy* (Doctoral dissertation, Technische Universität München).

Clancy, M. V., Zytynska, S. E., Senft, M., Weisser, W. W., & Schnitzler, J. P. (2016). Chemotypic variation in terpenes emitted from storage pools influences early aphid colonisation on tansy. *Scientific reports*, *6*(1).

Crutsinger, G. M., Collins, M. D., Fordyce, J. A., Gompert, Z., Nice, C. C., & Sanders, N. J. (2006). Plant genotypic diversity predicts community structure and governs an ecosystem process. *science*, *313*(5789), 966-968.

De Bello, F., Lavorel, S., Albert, C. H., Thuiller, W., Grigulis, K., Dolezal, J., & Lepš, J. (2011). Quantifying the relevance of intraspecific trait variability for functional diversity. Methods in *Ecology and Evolution, 2*(2), 163-174.

Dicke, M., Van Loon, J. J., & Soler, R. (2009). Chemical complexity of volatiles from plants induced by multiple attack. *Nature chemical biology*, *5*(5), 317-324.

Dudareva, N., Negre, F., Nagegowda, D. A., & Orlova, I. (2006). Plant volatiles: recent advances and future perspectives. *Critical reviews in plant sciences*, *25*(5), 417-440.

Eckert, S., Eilers, E. J., Jakobs, R., Anaia, R. A., Aragam, K. S., Bloss, T., & Mueller, C. (2023). Inter-laboratory comparison of plant volatile analyses in the light of intra-specific chemodiversity. *bioRxiv*, 2023-02.

Eilers, E. J. (2021). Intra-Individual and intraspecific terpenoid diversity in *Erodium cicutarium*. *Plants*, *10*(8).

Eilers, E. J., Kleine, S., Eckert, S., Waldherr, S., & Müller, C. (2021). Flower production, headspace volatiles, pollen nutrients, and florivory in *Tanacetum vulgare* chemotypes. *Frontiers in Plant Science*, *11*.

Erb, M., & Kliebenstein, D. J. (2020). Plant secondary metabolites as defenses, regulators, and primary metabolites: the blurred functional trichotomy. *Plant Physiology*, *184*(1), 39-52.

Fernandez-Conradi, P., Defossez, E., Delavallade, A., Descombes, P., Pitteloud, C., Glauser, G., Pellisier, L. & Rasmann, S. (2022). The effect of community-wide phytochemical diversity on herbivory reverses from low to high elevation. *Journal of Ecology*, 110(1), 46-56.

Fox J., & Weisberg, S. (2019). An {R} Companion to Applied Regression, Third Edition. Thousand Oaks CA: Sage.

Fridley, J. D., & Grime, J. P. (2010). Community and ecosystem effects of intraspecific genetic diversity in grassland microcosms of varying species diversity. *Ecology, 91*(8), 2272-2283.

Gallien, L. (2017). Intransitive competition and its effects on community functional diversity. *Oikos*, *126*(5), 615–623.

Genung, M. A., Bailey, J. K., & Schweitzer, J. A. (2012). Welcome to the neighbourhood: interspecific genotype by genotype interactions in Solidago influence above-and belowground biomass and associated communities. *Ecology Letters*, *15*(1), 65-73.

Guisan, A., Mod, H. K., Scherrer, D., Münkemüller, T., Pottier, J., Alexander, J. M., & d'Amen, M. (2019). Scaling the linkage between environmental niches and functional traits for improved spatial predictions of biological communities. *Global Ecology and Biogeography*, *28*(10), 1384-1392.

Harvey, J., Van Nouhuys, S., & Biere, A. (2005). Effects of quantitative variation in allelochemicals in *Plantago lanceolata* on development of a generalist and a specialist herbivore and their endoparasitoids. *Journal of Chemical Ecology*, *31,* 287-302.

Hauri, K. C., Glassmire, A. E., Randall, B., Zehr, L. N., & Wetzel, W. C. (2022). Plant chemical diversity and its frequency have distinct but complementary effects on insect foraging. *Journal of Applied Ecology, 59*(5), 1362-137

Hauri, K. C., Glassmire, A. E., & Wetzel, W. C. (2021). Chemical diversity rather than cultivar diversity predicts natural enemy control of herbivore pests. *Ecological Applications, 31*(3), e02289.

He, J., Chen, F., Chen, S., Lv, G., Deng, Y., Fang, W., Liu, Z., Guan, Z., & He, C. (2011). Chrysanthemum leaf epidermal surface morphology and antioxidant and defense enzyme activity in response to aphid infestation. *Journal of Plant Physiology*, *168*(7), 687–693.

Heil, M., & Karban, R. (2010). Explaining evolution of plant communication by airborne signals. *Trends in Ecology & Evolution*, *25*(3), 137-144.

Herms, D. A., & Mattson, W. J. (1992). The dilemma of plants: to grow or defend. *The Quarterly Review of Biology*, *67*(3), 283-335.

Himanen, S. J., Blande, J. D., Klemola, T., Pulkkinen, J., Heijari, J., & Holopainen, J. K. (2010). Birch (*Betula* spp.) leaves adsorb and re-release volatiles specific to neighbouring plants–a mechanism for associational herbivore resistance? *New Phytologist*, *186*(3), 722-732.

Hughes, A. R., Inouye, B. D., Johnson, M. T. J., Underwood, N., & Vellend, M. (2008). Ecological consequences of genetic diversity. *Ecology Letters, 11,* 609–623.

Isah, T. (2019). Stress and defense responses in plant secondary metabolites production. *Biological research*, *52*.

Isbell, F., Calcagno, V., Hector, A., Connolly, J., Harpole, W. S., Reich, P. B., & Loreau, M. (2011). High plant diversity is needed to maintain ecosystem services. *Nature*, *477*(7363), 199-202.

Junker, R. R., Blüthgen, N., & Keller, A. (2015). Functional and phylogenetic diversity of plant communities differently affect the structure of flower-visitor interactions and reveal convergences in floral traits. *Evolutionary Ecology*, *29,* 437-450.

Kabouw, P., van der Putten, W., van Dam, N., & Biere, A. (2010). Effects of intraspecific variation in white cabbage (Brassica oleracea var. capitata) on soil organisms. *Plant and Soil*, *336*, 509-518.

Karban, R., Yang, L. H., & Edwards, K. F. (2014). Volatile communication between plants that affects herbivory: A meta-analysis. *Ecology Letters*, *17*(1), 44-52.

Keskitalo, M., Lindén, A., & Valkonen, J. P. T. (1998). Genetic and morphological diversity of Finnish tansy (*Tanacetum vulgare* L., Asteraceae). *Theoretical and Applied Genetics*, *96*, 1141-1150.

Keskitalo, M., Pehu, E., & Simon, J. E. (2001). Variation in volatile compounds from tansy (*Tanacetum vulgare* L.) related to genetic and morphological differences of genotypes. *Biochemical Systematics and Ecology*, *29*(3), 267–285.

Kessler, A., & Kalske, A. (2018). Plant secondary metabolite diversity and species interactions. *Annual Review of Ecology, Evolution, and Systematics*, *49,* 115-138.

Kleine, S., & Müller, C. (2011). Intraspecific plant chemical diversity and its relation to herbivory. *Oecologia*, *166,* 175-186.

Kleine, S., & Müller, C. (2013). Differences in shoot and root terpenoid profiles and plant responses to fertilisation in *Tanacetum vulgare*. *Phytochemistry*, *96,* 123-131.

Koricheva, J., & Hayes, D. (2018). The relative importance of plant intraspecific diversity in structuring arthropod communities: A meta-analysis. *Functional Ecology*, *32*(7), 1704-1717.

Kos, M., Broekgaarden, C., Kabouw, P., Oude Lenferink, K., Poelman, E., Vet, L., & van Loon, J. (2011). Relative importance of plant-mediated bottom-up and top-down forces on herbivore abundance on Brassica oleracea. *Functional Ecology*, *25*(5), 1113-1124.

Kostenko, O., & Bezemer, T. (2013). Intraspecific variation in plant size, secondary plant compounds, herbivory and parasitoid assemblages during secondary succession. *Basic and applied ecology*, *14*(4), 337-346.

Kuppler, J., Höfers, M. K., Wiesmann, L., & Junker, R. R. (2016). Time-invariant differences between plant individuals in interactions with arthropods correlate with intraspecific variation in plant phenology, morphology and floral scent. *New Phytologist*, *210*(4), 1357-1368.

Mahdavi-Arab, N., Meyer, S. T., Mehrparvar, M., & Weisser, W. W. (2014). Complex effects of fertilization on plant and herbivore performance in the presence of a plant competitor and activated carbon. *Plos One*, *9*(7).

McCormick, A. C., Unsicker, S. B., & Gershenzon, J. (2012). The specificity of herbivore-induced plant volatiles in attracting herbivore enemies. *Trends in Plant Science*, *17*(5), 303-310.

Messier, J., McGill, B. J., & Lechowicz, M. J. (2010). How do traits vary across ecological scales? A case for trait-based ecology. *Ecology Letters*, *13*(7), 838-848.

Moore, B. D., Andrew, R. L., Külheim, C., & Foley, W. J. (2014). Explaining intraspecific diversity in plant secondary metabolites in an ecological context. *New Phytologist*, *201*(3), 733-750.

Moreira, X., Abdala-Roberts, L., Rasmann, S., Castagneyrol, B. & Mooney, K.A. (2016). Plant diversity effects on insect herbivores and their natural enemies: current thinking, recent findings, and future directions. *Current Opinion in Insect Science*, *14*, 1–7.

Müller, C., Bräutigam, A., Eilers, E., Junker, R., Schnitzler, J. P., Steppuhn, A. & Wittmann, M. (2020). Ecology and evolution of intraspecific chemodiversity of plants. *Research Ideas and Outcomes*, *6*.

Müller, C., & Junker, R. R. (2022). Chemical phenotype as important and dynamic niche dimension of plants. *New Phytologist, 234*(4), 1168-1174.

Neuhaus-Harr, A., Ojeda-Prieto, L., Eilers, E., Muller, C., Weisser, W. W., & Heinen, R. (2023). Chemodiversity affects preference for Tanacetum vulgare chemotypes in two aphid species. *bioRxiv*, 2023-03.

Ninkovic, V., Markovic, D., & Rensing, M. (2021). Plant volatiles as cues and signals in plant communication. *Plant, cell & environment*, *44*(4), 1030-1043.

Ninkovic, V., Rensing, M., Dahlin, I., & Markovic, D. (2019). Who is my neighbor? Volatile cues in plant interactions. *Plant Signaling & Behavior*, *14*(9).

Pang, Z., Chen, J., Wang, T., Gao, C., Li, Z., Guo, L., & Cheng, Y. (2021). Linking plant secondary metabolites and plant microbiomes: a review. *Frontiers in Plant Science*, *12*.

Petrén, H., Köllner, T. G., & Junker, R. R. (2023). Quantifying chemodiversity considering biochemical and structural properties of compounds with the R package chemodiv. *New Phytologist*, *237*(6), 2478-2492.

Poelman, E., Dam, N., Loon, J., Vet, L., & Dicke, M. (2009). Chemical diversity in *Brassica oleracea* affects biodiversity of insect herbivores. *Ecology*, *90*(7), 1863-1877.

Raffard, A., Santoul, F., Cucherousset, J., & Blanchet, S. (2019). The community and ecosystem consequences of intraspecific diversity: A meta-analysis. *Biological Reviews*, *94*(2), 648-661.

Rashid, M., & Chung, Y. R. (2017). Induction of systemic resistance against insect herbivores in plants by beneficial soil microbes. *Frontiers in Plant Science*, *8*.

Rohloff, J., Mordal, R., & Dragland, S. (2004). Chemotypical variation of tansy (*Tanacetum vulgare* L.) from 40 different locations in Norway. *Journal of Agricultural and Food Chemistry*, *52*(6), 1742-1748.

Russell, V. L. (2021). Emmeans: Estimated Marginal Means, aka Least-Squares Means. R package version 1.7.1-1.

Senft, M., Weisser, W. W., & Zytynska, S. E. (2017). Habitat variation, mutualism and predation shape the spatio-temporal dynamics of tansy aphids. *Ecological Entomology*, *42*(4), 389-401.

Siefert, A., Violle, C., Chalmandrier, L., Albert, C. H., Taudiere, A., Fajardo, A., & Wardle, D. A. (2015). A global meta-analysis of the relative extent of intraspecific trait variation in plant communities. *Ecology Letters*, *18*(12), 1406-1419.

Takabayashi, J., Dicke, M., & Posthumus, M. A. (1994). Volatile herbivore-induced terpenoids in plant-mite interactions: variation caused by biotic and abiotic factors. *Journal of Chemical Ecology*, *20*, 1329-1354.

Tilman, D., Lehman, C. L., & Thomson, K. T. (1997). Plant diversity and ecosystem productivity: theoretical considerations. *Proceedings of the National Academy of Sciences*, *94*(5), 1857-1861.

Viola, D. V., Mordecai, E. A., Jaramillo, A. G., Sistla, S. A., Albertson, L. K., Gosnell, J. S., & Levine, J. M. (2010). Competition–defense tradeoffs and the maintenance of plant diversity. *Proceedings of the National Academy of Sciences*, *107*(40), 17217-17222.

Violle, C., Enquist, B. J., McGill, B. J., Jiang, L. I. N., Albert, C. H., Hulshof, C., & Messier, J. (2012). The return of the variance: intraspecific variability in community ecology. *Trends in Ecology & Evolution*, *27*(4), 244-252.

Weisser, W. W., Roscher, C., Meyer, S. T., Ebeling, A., Luo, G., Allan, E., & Eisenhauer, N. (2017). Biodiversity effects on ecosystem functioning in a 15-year grassland experiment: Patterns, mechanisms, and open questions. *Basic and applied ecology*, *23*, 1-73.

Westerband, A. C., Funk, J. L., & Barton, K. E. (2021). Intraspecific trait variation in plants: a renewed focus on its role in ecological processes. *Annals of Botany*, *127*(4), 397-410.

Wetzel, W. C., & Whitehead, S. R. (2020). The many dimensions of phytochemical diversity: linking theory to practice. *Ecology Letters*, *23*(1), 16-32.

Wickham, H. (2016). Ggplot2: Elegant Graphics for Data Analysis. Springer-Verlag New York.

Wurst, S., Van Dam, N. M., Monroy, F., Biere, A., & Van der Putten, W. H. (2008). Intraspecific variation in plant defense alters effects of root herbivores on leaf chemistry and aboveground herbivore damage. *Journal of chemical ecology*, *34*, 1360-1367.

Zhou, H., Hua, J., Zhang, J., & Luo, S. (2022). Negative Interactions Balance Growth and Defense in Plants Confronted with Herbivores or Pathogens. *Journal of Agricultural and Food Chemistry*, *70*(40), 12723-12732.

Ziaja, D., & Mueller, C. (2022). Intraspecific chemodiversity provides plant individual-and neighbourhood-mediated associational resistance towards aphids. *bioRxiv*, 2022-12.

Figures

Figure 1

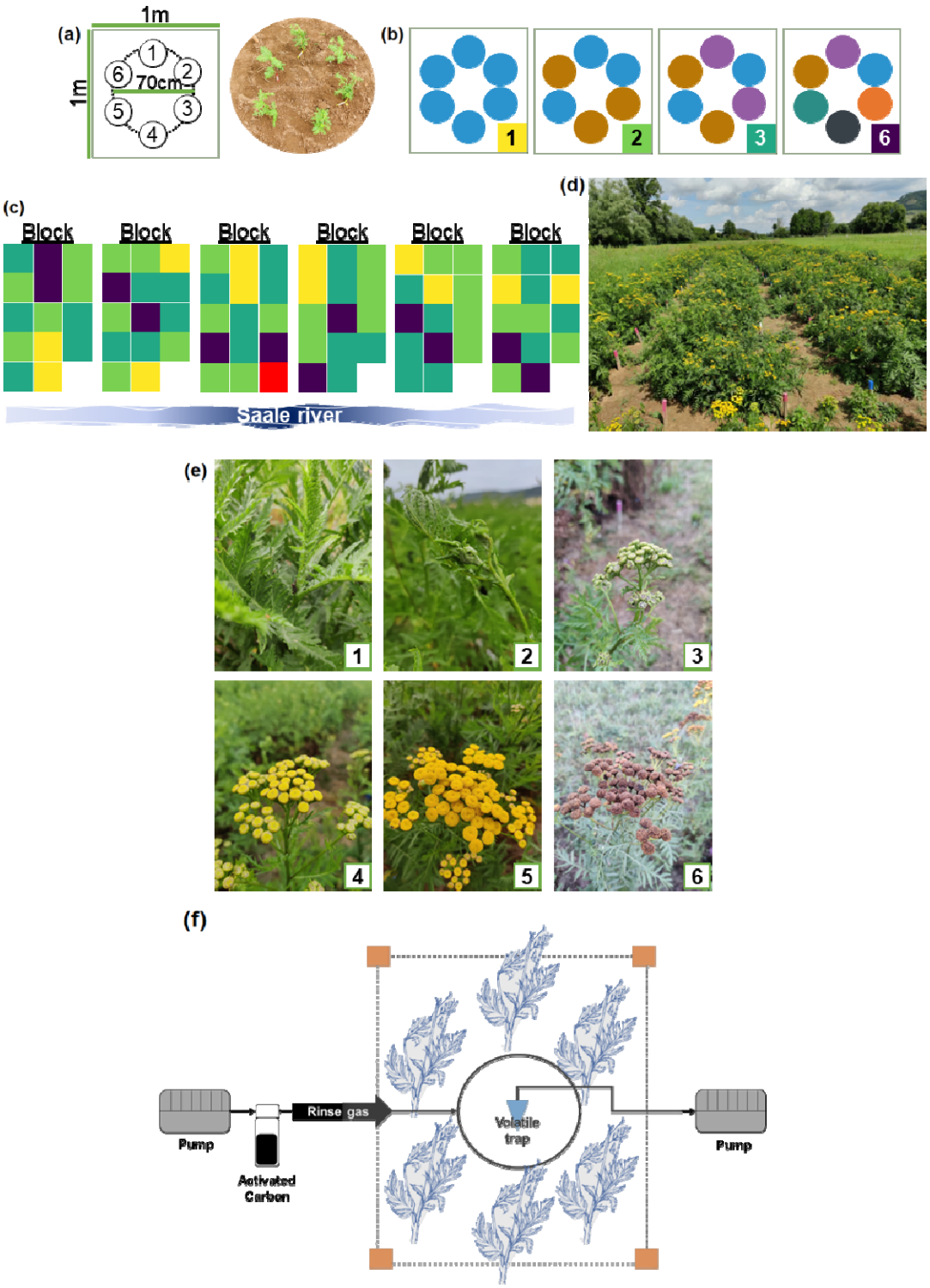

Figure 1: Field experimental design. Plant arrangement within the plot: six *T. vulgare* plants were evenly distributed around a 70 cm diameter circle. The identity of tansy chemotypes in each plot was assigned to plots *a priori*, and plot position was assigned randomly **(a)**. Plot-level chemotype richness: The number of different chemotypes in one plot ranged from 1, 2, 3, to 6 **(b)**. Block design showing plot-level chemotype richness, reflected by yellow, light green, dark green and purple squares, indicating plot-level chemotype richness (1, 2, 3, and 6, respectively). N = 84 plots were distributed equally in six randomized blocks. Each block consisted of 14 plots: two plots of chemotype richness level 1, five plots each of chemotype richness level 2 and 3, and two plots with chemotype richness level 6. The red plot indicates the location of the background volatile profile plot **(c)**. Picture of the field in June 2021 **(d)**. Stem phenology (*left-to-right then top-to-bottom*): No flowering stem [1], Developing closed flowering stem [2], Developing open flowering stem [3], Unripe flowering stem [4], Ripe flowering stem [5], Stem with mature seeds [6] **(e)**. Closed-push-pull headspace VOC collection system. Pressurized purified air enters the collection PET bag, and it is pulled through a volatile trap located in the middle of the 6 plants at the higher side of the bag **(f)**.

Figure 2

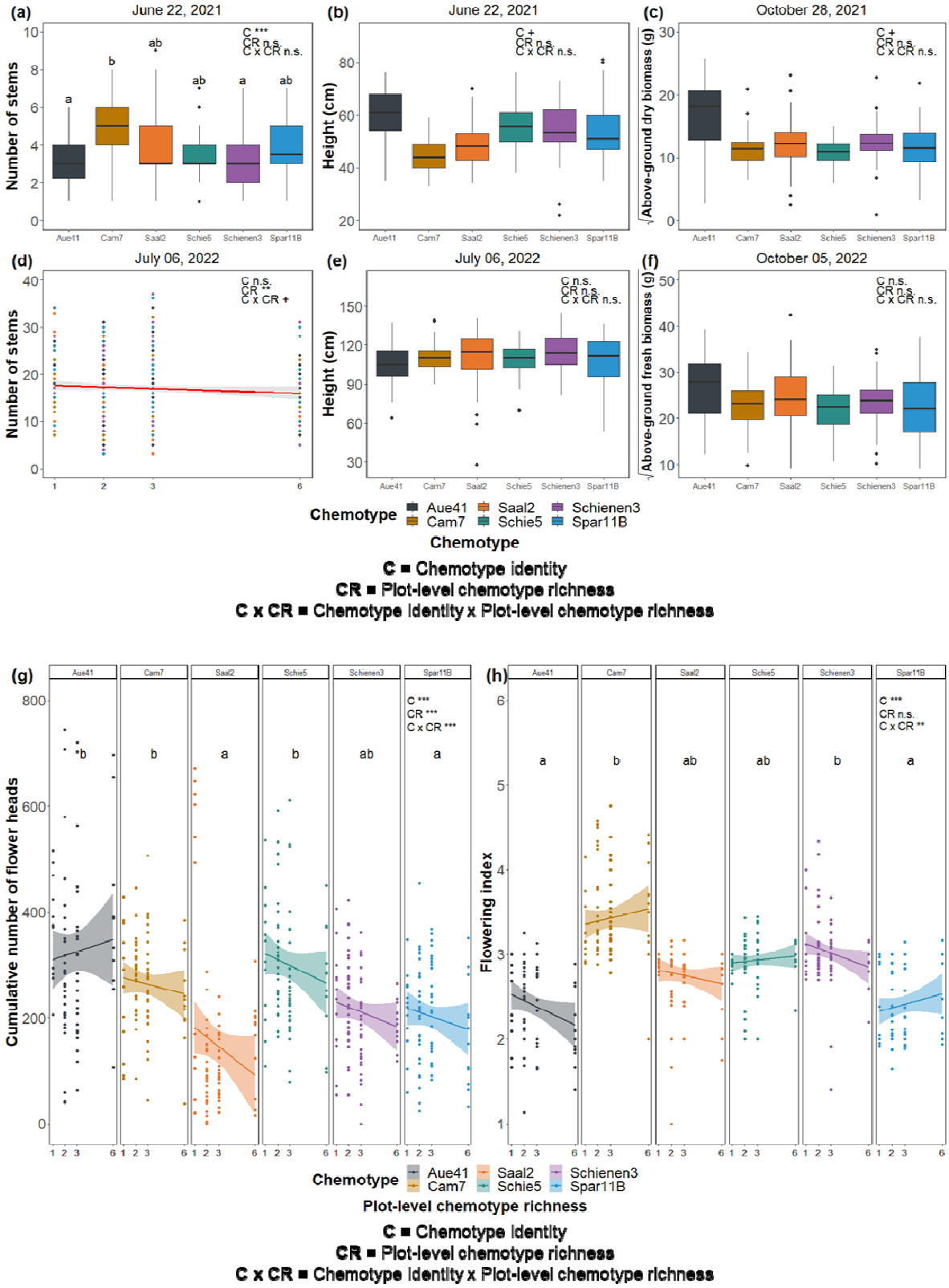
(a)
June 22, 2021
C ***
CR n.s.
C x CR n.s.
Number of stems
(b)
June 22, 2021
C +
CR n.s.
C x CR n.s.
Height (cm)
(c)
October 28, 2021
C +
CR n.s.
C x CR n.s.
√Above-ground dry biomass (g)
(d)
July 06, 2022
C n.s.
CR **
C x CR +
Number of stems
(e)
July 06, 2022
C n.s.
CR n.s.
C x CR n.s.
Height (cm)
(f)
October 05, 2022
C n.s.
CR n.s.
C x CR n.s.
√Above-ground fresh biomass (g)
Aue41 Cam7 Saal2 Schie5 Schienen3 Spar11B
Chemotype
Aue41 Cam7 Saal2 Schie5 Schienen3 Spar11B
Chemotype
C = Chemotype identity
CR = Plot-level chemotype richness
C x CR = Chemotype identity x Plot-level chemotype richness
(g)
C ***
CR ***
C x CR ***
Cumulative number of flower heads
(h)
C ***
CR n.s.
C x CR **
Flowering index
Chemotype
Aue41 Cam7 Saal2 Schie5 Schienen3 Spar11B
Plot-level chemotype richness
C = Chemotype identity
CR = Plot-level chemotype richness
C x CR = Chemotype identity x Plot-level chemotype richness

Figure 2: Effect of chemotype identity (C) and plot-level chemotype richness (CR) on growth traits of *T. vulgare* in 2021: Number of stems **(a)**, height (cm) **(b)**, and square root dry above-ground biomass (g) **(c)**. Effect of chemotype (C) and plot-level chemodiversity (CR) on growth traits of *T. vulgare* in 2022: Number of stems **(d)**, height (cm) **(e)**, and square root fresh above-ground biomass (g) **(f)**. **Effect of chemotype identity (C) and plot-level chemodiversity (CR) on reproductive traits of *T. vulgare*:** Cumulative number of flower heads in 2021 **(g)**, and flowering index in 2022 **(h)**. Significance is indicated as follows: **n.s.** = not significant, **+** p = 0.05 - 0.10, ***** p <0.05, ****** p <0.01 and ******* p <0.001. Degrees of freedom, Chi-square, and p-values are reported in Table 1. Tukey *post hoc* significant differences are indicated with different letters.

Figure 3

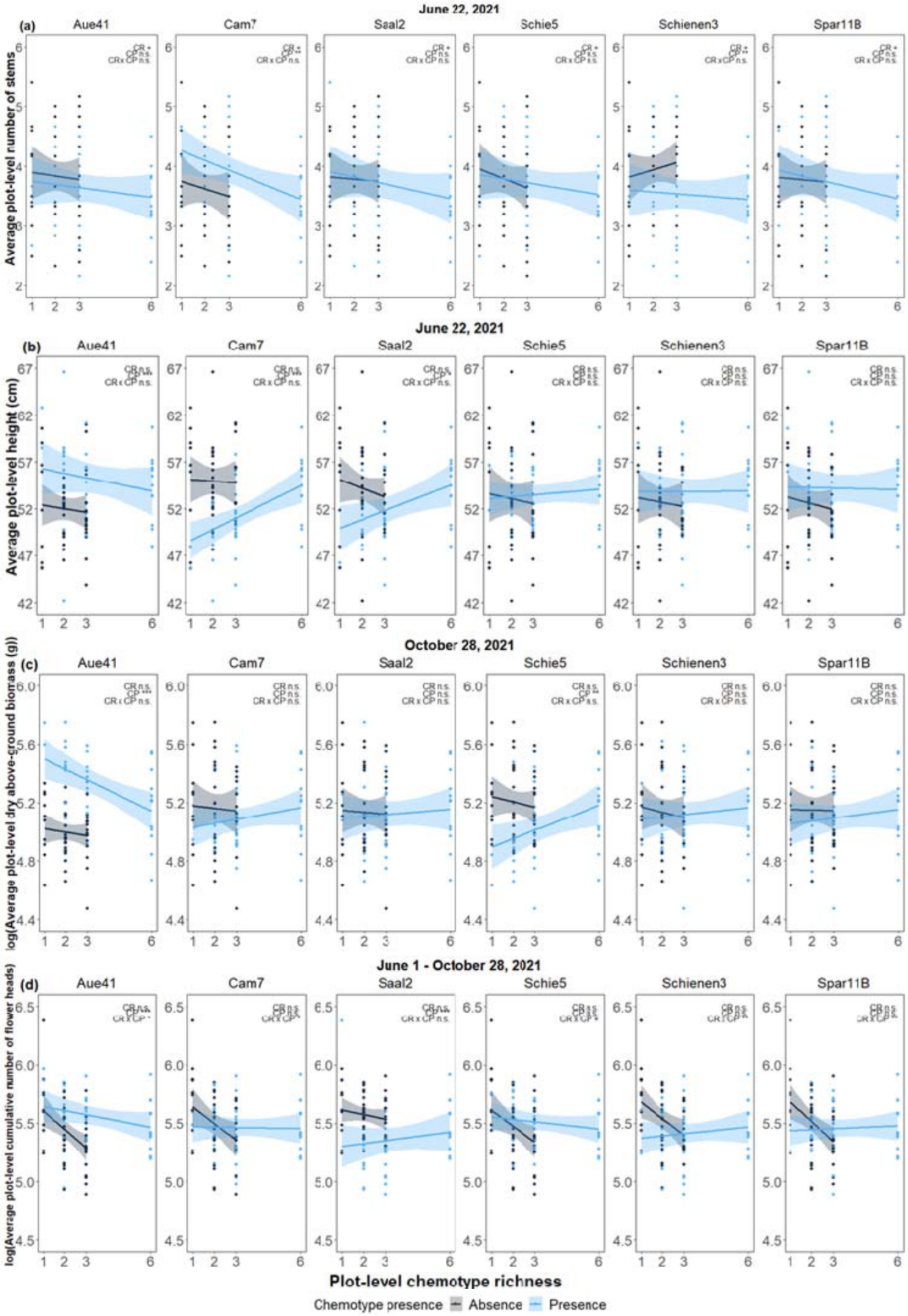

CR = Plot-level chemotype richness
CP = Chemotype presence
CR x CP = Plot-level chemotype richness x Chemotype presence

Figure 3: Effect of chemotype presence (CP) and plot-level chemotype richness (CR) on average plot-level traits of *T. vulgare* in 2021: Number of stems **(a)**, height (cm) **(b)**, the logarithm of dry above-ground biomass **(c)**, and the logarithm of the cumulative number of flower heads **(d)**. Significance is indicated as follows: **n.s.** = not significant, **+** p = 0.05 - 0.10, ***** p <0.05, ****** p <0.01 and ******* p <0.001. Degrees of freedom, F-statistics, and p-values are reported in Table 2.

Figure 4

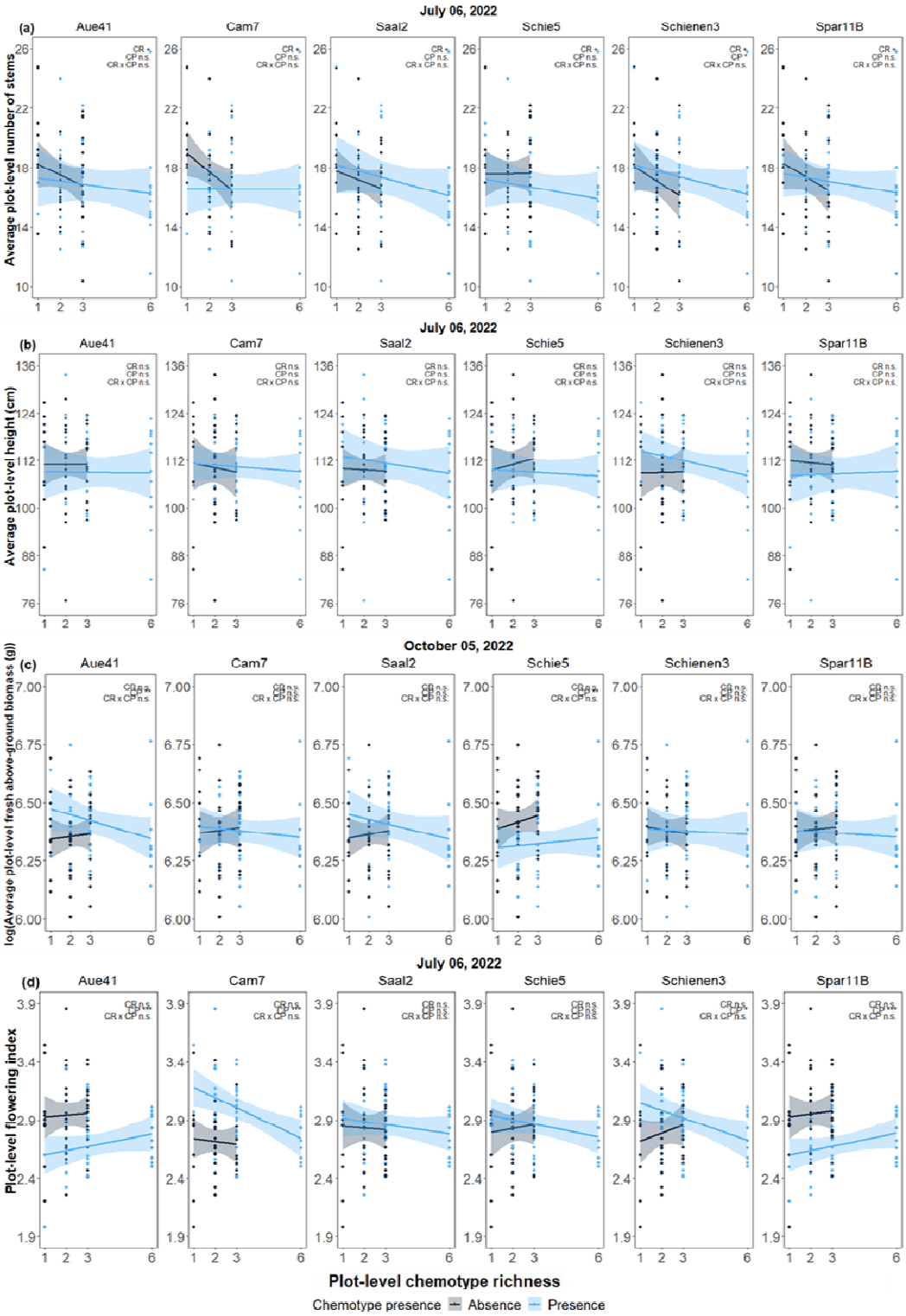

CR = Plot-level chemotype richness
CP = Chemotype presence
CR x CP = Plot-level chemotype richness x Chemotype presence

Figure 4: Effect of chemotype presence (CP) and plot-level chemotype richness (CR) on average plot-level traits of *T. vulgare* in 2022: Number of stems **(a)**, height (cm) **(b)**, the logarithm of fresh above-ground biomass (g) **(c)**, and flowering index **(d)**. Significance is indicated as follows: **n.s.** = not significant, **+** p = 0.05 - 0.10, ***** p <0.05, ****** p <0.01 and ******* p <0.001. Degrees of freedom, F-statistics, and p-values are reported in Table 2.

Figure 5

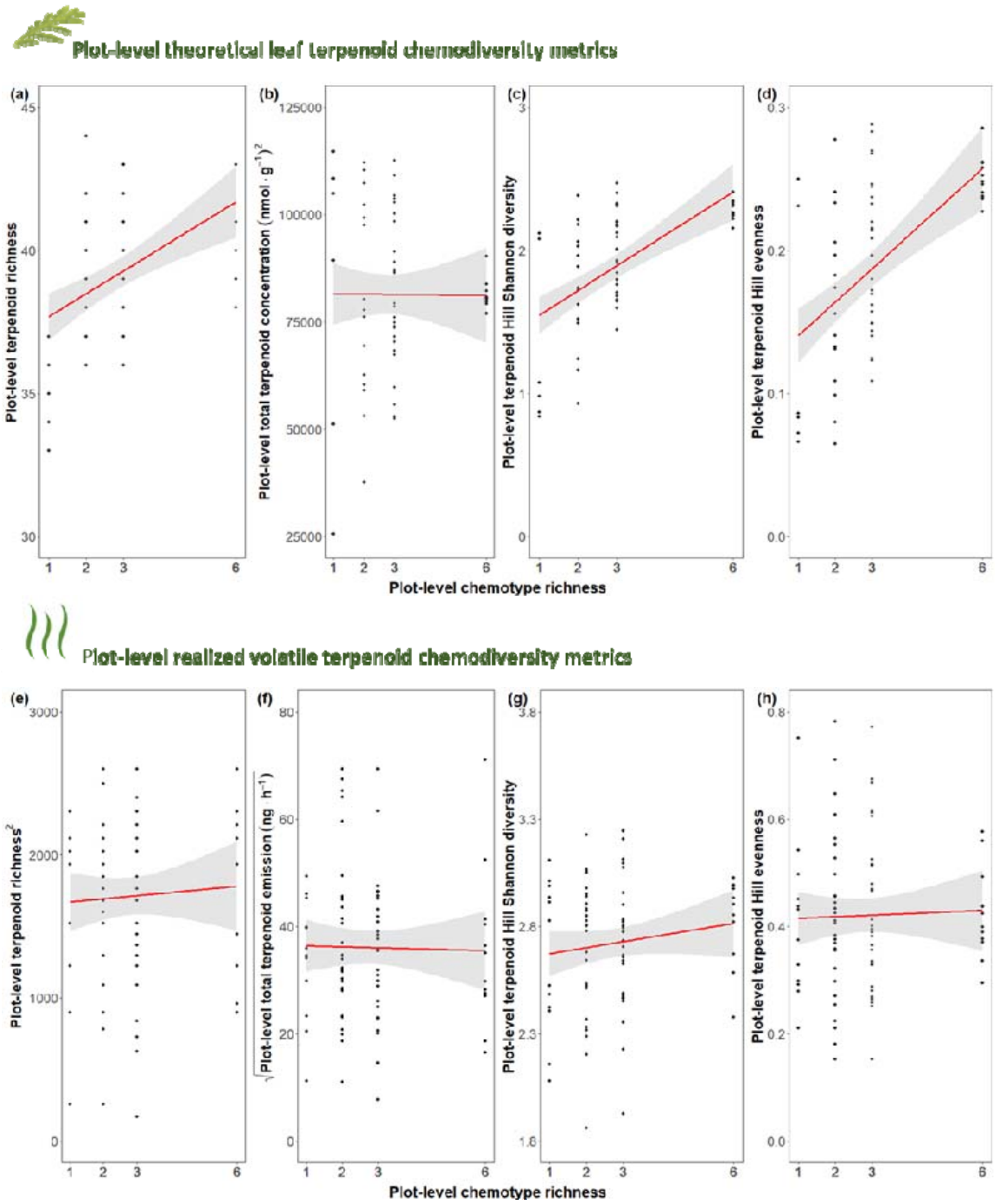
Plot-level theoretical leaf terpenoid chemodiversity metrics
(a)
(b)
(c)
(d)
Plot-level terpenoid richness
Plot-level total terpenoid concentration (nmol · g⁻¹)²
Plot-level terpenoid Hill Shannon diversity
Plot-level terpenoid Hill evenness
Plot-level chemotype richness
Plot-level realized volatile terpenoid chemodiversity metrics
(e)
(f)
(g)
(h)
Plot-level terpenoid richness²
√Plot-level total terpenoid emission (ng · h⁻¹)
Plot-level terpenoid Hill Shannon diversity
Plot-level terpenoid Hill evenness
Plot-level chemotype richness

Figure 5: The effects of plot-level chemotype richness on theoretical plot-level chemodiversity metrics based on leaf terpenoid profiles (a-d) and on realized plot-level volatile chemodiversity metrics (e-h). Theoretical plot-level leaf terpenoid diversity metrics were calculated by summing up the absolute leaf terpenoid concentrations (nmol/g) of each chemotype/daughter present in each plot, based on the chemical analysis of leaves from greenhouse plants in 2020 (Neuhaus-Harr *et al*., 2023). Realized plot-level volatile chemodiversity was based on terpenoids collected in the headspace (ng/h) in May 2022. Diversity metrics were calculated using the '*chemodiv'* package (Pétren *et al*., 2022). Plot-level chemotype richness effects on; plot-level theoretical terpenoid richness ($F_{1,82}$ = 20.48, R^2 = 0.20, p <0.001) **(a)**; squared plot-level theoretical total terpenoid concentration (nmol/g) ($F_{1,82}$ = 0.00, R^2 = 0.00, p = 0.967) **(b)**; plot-level theoretical terpenoid Hill Shannon index ($F_{1,82}$ = 37.25, R^2 = 0.31, p <0.001) **(c)**; and plot-level theoretical terpenoid Hill evenness ($F_{1,82}$ = 31.78, R^2 = 0.28, p <0.001) **(d)**; squared plot-level realized volatile terpenoid richness (χ^2_1 = 0.36, R^2 = 0.00, p = 0.546) **(e)**, square root of plot-level realized total volatile terpenoid emission (ng/h) (χ^2_1 = 0.02, R^2 = 0.00, p = 0.897) **(f)**, plot-level realized volatile terpenoid Hill Shannon index (χ^2_1 = 1.60, R^2 = 0.02, p = 0.206) **(g)**, and plot-level realized volatile terpenoid Hill evenness (χ^2_1 = 0.08, R^2 = 0.00, p = 0.780) **(h)**.